

Effect of Heating Rates on the Synthesis of Al_2O_3 -SiC Composites by the Self-Propagating High-Temperature Synthesis (SHS) Technique

Lokesh Chandra Pathak, Debajyoti Bandyopadhyay, Srinivasan Srikanth, Swapan Kumar Das, and P. Ramachandrarao

National Metallurgical Laboratory, Jamshedpur 831 007, India

Various aspects of *in situ* formation of Al_2O_3 -SiC composites by the self-propagating high-temperature synthesis (SHS) technique have been investigated using thermal analyses (TG/DTA) of a powder mixture (4Al, 3SiO₂, 3C) and pellets in an argon atmosphere at different heating rates. Both the reaction initiation and peak temperatures are found to increase with the heating rates. At lower heating rates, the powder samples do not reveal any exothermic peak possibly because of poor reactivity and sluggish exothermic reaction. The appearance of exothermic peaks in the DTA plots after melting of aluminum indicates reduction of silica by liquid aluminum. Conversion of aluminum is found to decrease marginally with an increase in heating rates. The apparent activation energy of the process compares well with the interdiffusion activation energy of silicon and oxygen, indicating that oxygen diffusion in Si formed at the reaction front may be the rate-controlling factor for this SHS process. From SEM studies it appears that the formation of SiC whiskers is through liquid-phase mass transfer.

I. Introduction

ALUMINA-BASED ceramic-matrix composites have shown promise as advanced materials for high-temperature applications because of their excellent refractoriness, low susceptibility to oxidation, and good mechanical properties at elevated temperatures.^{1–4} Besides the conventional powder metallurgical route, synthesis of these composites by *in situ* fabrication methods is gaining momentum due to certain inherent advantages. *In situ* fabrication techniques eliminate the problems of using fine ceramics, particularly whiskers, and the chances of segregation of the constituents are relatively low compared with mechanical mixing methods. There are also fewer processing steps in this route. Several techniques for the synthesis of *in situ* composites have been reported in the literature.^{5–8}

A new combustion synthesis technique for the fabrication of Al_2O_3 -SiC_w *in situ* composite using a rapid-heating self-propagating high-temperature synthesis (RH-SHS) has recently been reported by the authors.^{8,9} During synthesis of composites through the SHS technique, heating rates may have a significant influence on the reaction initiation temperature (T_i), the mechanism of the combustion reaction, as well as the quality of the products.^{10–12} The synthesis of Ti-Al intermetallic compounds by the SHS route has shown that the mechanism of the reaction changes from solid-liquid interaction to solid-solid interaction with an increase in the heating rates.¹² It has also been reported that an increase in the heating rates improves the density of the SHS product.¹¹

The RH-SHS technique has shown the feasibility of fabrication of Al_2O_3 -SiC *in situ* composites,^{8,9} but several aspects, which include heating rates, green density, composition, etc., have not yet been investigated. In this paper, an attempt has been made to investigate the influence of heating rates on the synthesis of Al_2O_3 -SiC composites.

II. Experimental Procedure

Stoichiometric amounts of silica (SiO₂) (99% pure), aluminum (99% pure), and carbon (graphite, 98% pure) powders in 4:3:1 molar ratio were taken in a stainless steel container and milled for 6 h. Approximately 6 g of milled powder mixture was pressed to 2.5 cm diameter pellets at a pressure of ≈ 100 MPa. Approximately 1 wt% of poly(vinyl alcohol) (PVA) was added as a binder during pelletization. The green pellets were dried at 150°C for 3 h to remove the moisture.

Simultaneous differential thermal analyses (DTA) and thermogravimetric analyses (TGA) of the powder mixture and the pellets were conducted in a Seiko TG/DTA apparatus (Model No. 320). The average particle size of the powder sample was 30 μm and the green densities of the pellets were found to be 60% of the theoretical density. Before the thermal analysis experiments, the sample chamber was flushed with pure argon gas ($\text{O}_2 \sim 2$ ppm) and the investigations were conducted under continuous flow of argon gas at a rate of 50 mL/min. The samples were heated from the ambient temperature to 1200°C at several heating rates ranging between 5 and 100°C/min. On attainment of the desired temperatures the samples were cooled down to room temperature. The experimental conditions used for this study are summarized in Table I. The reaction initiation temperature (T_i) was measured from the DTA plots using the three-point method. The time interval between T_i and the exothermic peak temperature, T_p , was noted. In one of the experiments, the pellet was heated at a rate of 400°C/min from ambient temperature to 1450°C and soaked for 10 min in a graphite furnace. Then the pellet was furnace cooled and characterized.

The samples were characterized by XRD, SEM, and energy-dispersive X-ray spectroscopy (EDS). XRD analyses of the samples were conducted at different stages of processing. Fractured surfaces of the samples were studied with a JEOL-840A SEM system equipped with a Kevex EDS system.

III. Results and Discussion

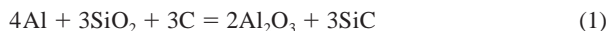
In the combustion synthesis technique, the self-sustainability of the exothermic reaction and the propagation of a combustion wave front mostly depend on the enthalpy change associated with the reaction and the rate of energy dissipation from the system.^{13,14} The adiabatic temperature, T_{ad} , indicates that the maximum temperature attained by the products under adiabatic conditions is an important SHS parameter. It has been reported that a value T_{ad} above 1800 K is required for the self-sustainability of the exothermic reaction.^{14,15} It is also well known that most of the exothermic

N. S. Jacobson—contributing editor

Table I. Details of the Experimental Conditions

Sample	Sample mass (mg)	Form	Heating rate (°C/min)	Final temperature (°C)
P ₁	15.941	Powder	10	1200
P ₂	14.578	Powder	40	1200
P ₃	16.892	Powder	100	1200
C ₁	25.982	Pellet	5	1200
C ₂	47.893	Pellet	10	1200
C ₃	48.451	Pellet	20	1200
C ₄	38.734	Pellet	40	1200
C ₅	32.091	Pellet	60	1200
C ₆	37.955	Pellet	80	1200
C ₇	34.351	Pellet	100	1200
C ₈	5.0 g	Pellet	400	1450

reactions are initiated at a temperature (T_i) above room temperature. T_{ad} for the reaction



was calculated to be 2375 K based on the thermodynamic data from a recent compilation.¹⁶ The high value of the adiabatic temperature of the reacting system under consideration suggests the possibility of self-sustenance of the reaction propagation and simultaneous sintering of the SHS products.

(I) Thermal Analysis

(A) *Powder System:* DTA plots for the stoichiometric powder mixture of Al + SiO₂ + C (in 4:3:1 molar ratio) heated at various rates of 10, 40 and 100°C/min are shown in Fig. 1(a). A small endothermic peak appears at 572°C followed by a major endothermic peak at 660°C (Fig. 1(a)). The first endothermic peak is due to the transformation of SiO₂ from α - to β -phase and the second one represents the melting of aluminum. Except for these two peaks, no other peak could be noticed in the thermogram of sample P₁ (heating rate = 10°C/min) in the temperature range of observation. However, for powder sample P₃ heated at a rate of 100°C/min, two additional exothermic peaks at \approx 890°C and at \approx 1100°C are observed. These exothermic peaks are likely to be due to the formation of aluminum oxide and SiC, respectively (Fig. 1(c)). The absence of an exothermic peak for sample P₁ can possibly be attributed to the poor contact between the reacting components in the powdered samples. The segregation of liquid Al during slow heating might have also hindered the combustion

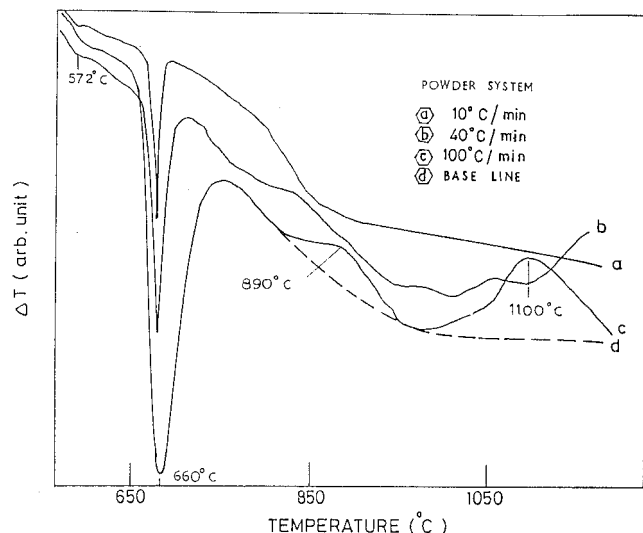


Fig. 1. DTA thermogram of the powder samples P₁ (a), P₂ (b), and P₃ (c). Comparing the effect of heating rates on the various transformations during the combustion synthesis of composites (the broken line implies the base line, d).

reaction. In the case of sample P₃ (Fig. 1(c)), even though the contact is poor, a higher rate of heat input appears to catalyze the exothermic reactions at localized zones, resulting in exothermic peaks in the thermograms.

(B) *Pellets:* A representative DTA plot for pellet sample C₂ heated at a rate of 10°C/min is shown in Fig. 2. Similar to the powder samples, two endothermic peaks are observed to initiate at 572° and 660°C in the DTA thermograms. Besides these endothermic peaks, exothermic peaks are also observed in the thermograms for all of the heating rates. The appearance of prominent exothermic peaks above 720°C in the pellets is due to better contact between the reactant constituents. The shift of the exothermic peaks toward higher temperature sides for samples C₁, C₃, and C₆ are shown in Fig. 3, which indicates that both the reaction initiation temperature (T_i) and the peak temperature (T_p) increase with an increase in the heating rates.

The exothermic peaks occurring just after the melting of aluminum appear to be a superimposition of three exothermic reactions. These overlapped peaks become more distinguishable at higher heating rates. TG/DTA plots of pellet C₇ with three deconvoluted (using Gaussian fitting) DTA peaks are shown in Fig. 4. The first exothermic peak is due to the aluminothermic reduction of silica, i.e.,



and the second peak is due to the reaction of Si and C forming SiC i.e.,



The third exothermic peak may be due to the oxidation of Al, Si, or SiC by the traces of oxygen present in argon. The weight gain of the sample as observed from the TG plot (Fig. 4) and the peak of the differential thermogravimetry (DTG) plot (not shown in the figure) strongly suggest an oxidation phenomenon.

The variations of T_i and T_p with heating rates for the aluminothermic reduction of silica are shown in Fig. 5. The reaction initiation temperature at a low heating rate, i.e., 5°C/min, is observed to be 723°C, which matches well with the reported value of 715–720°C in the literature.⁷ The variation of the second exothermic peak temperature, $T_{p(\text{SiC})}$, for SiC formation as a function of heating rate is also shown in Fig. 5. It can also be observed that $T_{p(\text{SiC})}$ increases continuously with an increase of heating rates and the lowest peak temperature for SiC formation is noted to be 867°C for pellet sample C₂. The formation of SiC well

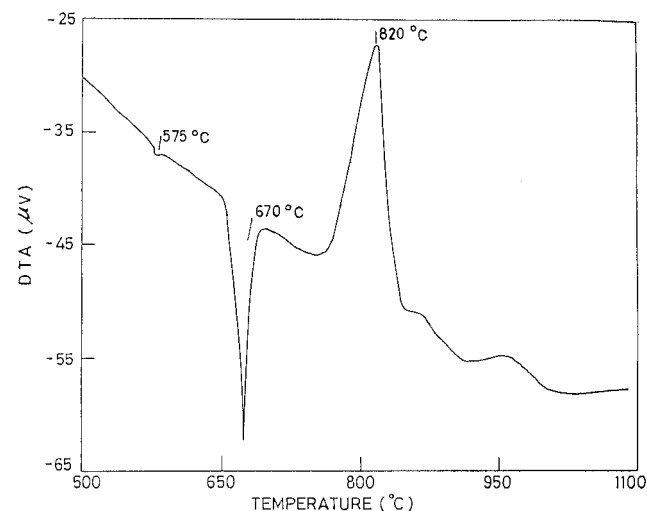


Fig. 2. Typical DTA plot of the compact C₂ heated at 10°C/min. The two endothermic peaks correspond to the $\alpha \rightarrow \beta$ transition in quartz and the exothermic peaks correspond to the formation of Al₂O₃ and SiC, respectively.

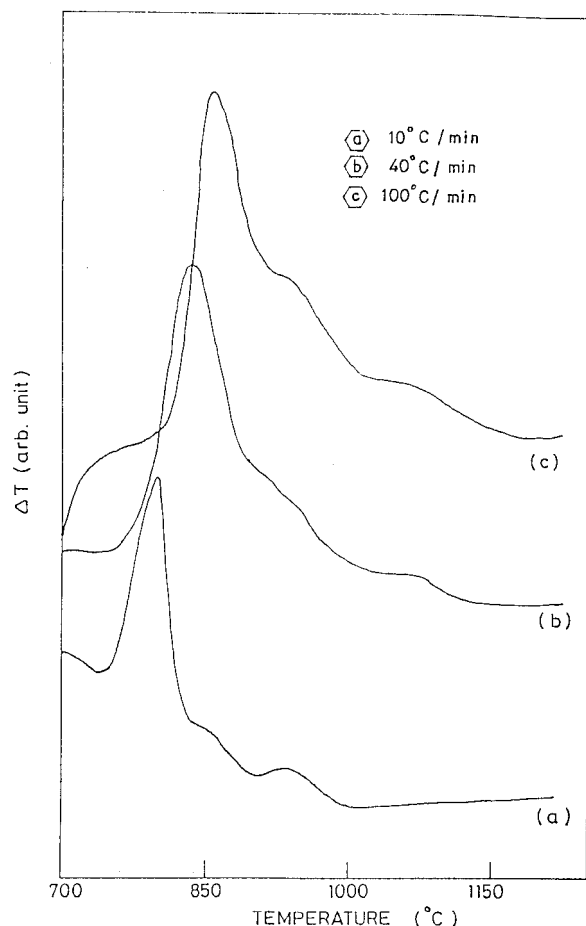


Fig. 3. Plot showing the shift of the exothermic peak with the heating rates for the pellets heated at (a) 10°C/min, (b) 40°C/min, and (c) 100°C/min.

below the reported value of the ignition temperature (1425°C)¹⁷ is possibly due to the localized attenuation of high temperature.

As mentioned, the aluminothermic reduction of SiO₂ is observed to be initiated at temperatures ≥723°C, higher than the melting point of aluminum (660.4°C). Poor wettability of liquid Al on SiO₂ may be one of the reasons for the higher reaction initiation temperature. Yi *et al.*¹² have reported that the liquid wetting mechanism operating in the SHS of the Ti-Al system is caused in lowering the reaction initiation temperature with the increase of the heating rate. However, the present investigation does not follow the findings of Yi *et al.*, possibly because of poor wettability. During the cooling cycle of the pellets after attainment of 1200°C, a minor exothermic peak could be observed at 545°C. The exothermic peak is due to solidification of unreacted aluminum at undercooled temperature. The ratio of the area of the endothermic peak in the heating cycle and the exothermic peak of the cooling cycle can be used to derive information on the amount of unreacted aluminum in the process.

Thermogravimetric analyses of the pellets show that there is around 1.1% to 1.4% increase in weight of the samples during heating. This increase can be attributed primarily to the oxidation of either Al, Si, or SiC by the traces of oxygen (~2 ppm) present in Ar. It is also observed that practically no weight gain can be noted up to 661°C, i.e., the melting point of aluminum. The weight gain is also found to be independent of the heating rates.

(2) Kinetic Analysis

Assuming that no appreciable change in the weight of the sample occurs during cooling and that the melting and freezing occur within a close temperature range, the heat equation can be expressed as

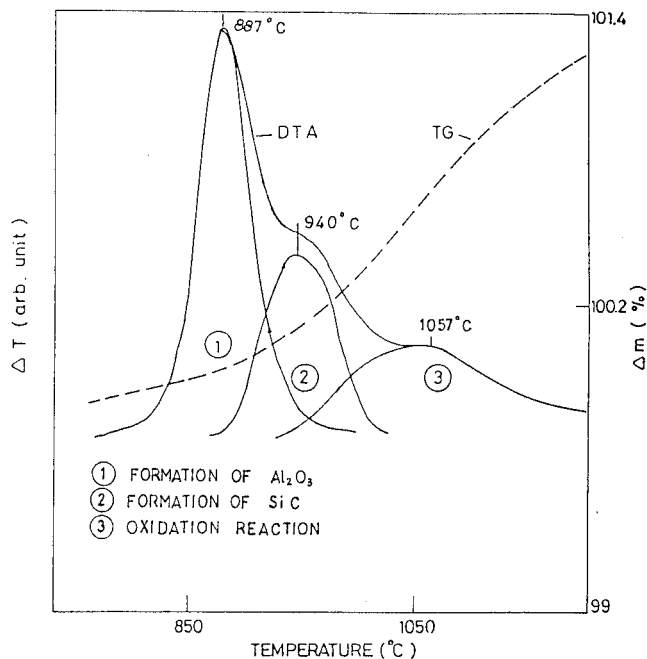


Fig. 4. Deconvoluted exothermic peak of sample C₇ showing the occurrence of three exothermic peaks. The peaks correspond to (1) formation of Al₂O₃, (2) formation of SiC, and (3) possible oxidation of the constituents.

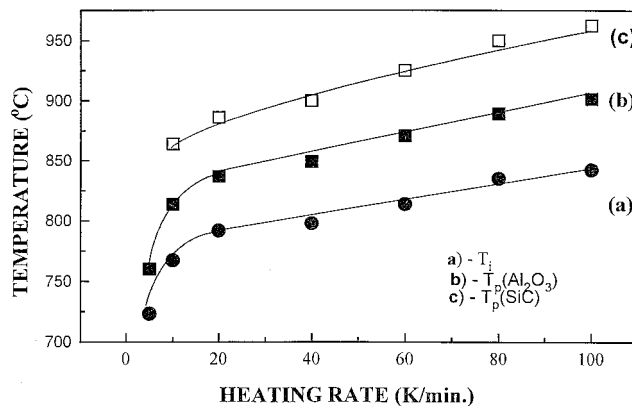


Fig. 5. Variation of reaction initiation temperature (*T_i*) (a) and peak temperature (*T_p*) of aluminum oxidation (b) and formation of silicon carbide (c), with the heating rates for the pellets.

$$Q_1 = m_1L \tag{4}$$

$$Q_2 = -m_2L \tag{5}$$

where *m*₁ and *m*₂ are the weight of the initial and unreacted aluminum, respectively, *Q*₁ and *Q*₂ are the total heat absorbed and evolved for aluminum melting and solidification, respectively, and *L* is the latent heat of fusion of Al per unit weight. From Eqs. (4) and (5), it can be deduced that

$$Q_1/Q_2 = m_1/m_2 = A_1/A_2 \tag{6}$$

assuming the machine constant (proportionality constant) and the mass of the system to be identical for the heating and cooling cycles. Here, *A*₁ and *A*₂ are the areas of the peaks for melting and solidification of aluminum, respectively. The fraction of aluminum reacted *f* can be expressed as

$$f = \frac{m_1 - m_2}{m_1} = 1 - \frac{A_2}{A_1} \tag{7}$$

Using Eq. (7), the fractions of aluminum reacted as a function of heating rates were calculated and are presented in Table II. It is apparent from the table that aluminum conversion to alumina has a marginal negative dependence over the heating rates. This observation can be explained in the light of the kinetics of reaction. A higher heating rate, although it increases the rate of heat input, decreases the time available for reaction. Transport of reactants, wetting, and chemical reaction all being time-dependent phenomena, scarcity of time is thus expected to lower the conversion of aluminum.

Table II also incorporates the time lapse between the initiation of the major exothermic reaction and attainment of peak temperature. This time is considered to be the effective time for exothermic reaction, assuming no significant conversion of reactants beyond T_p . It has been noticed that the reaction time decreases with an increase in heating rates. At high heating rates, the number of reacting molecules acquiring energy to overcome the activation energy barrier per unit time increases, resulting in a lowering of the reaction time.

The most extensively used expression for determination of the apparent activation energy of reaction in DTA is proposed by Kissinger and can be expressed as¹⁸

$$\beta/T_p^2 = ke^{-E/RT_p} \quad (8)$$

where β is the heating rate, T_p is the peak temperature in kelvins, E is the activation energy, k is the preexponential factor, and R is the gas constant. A plot of $\ln(\beta/T_p^2)$ as a function of the inverse of peak temperature ($1/T_p$) for the aluminothermic reduction of silica is presented in Fig. 6(a). The apparent activation energy for the aluminothermic reduction process is calculated from the slope of this linear plot and has been found to be 240 ± 5 kJ/mol. The estimated apparent activation energy is observed to match extremely well with the interdiffusion activation energy of Si and oxygen (241.7 kJ/mol).¹⁹ This suggests that reduction of silica by liquid aluminum in the present investigation is possibly controlled by the diffusion of oxygen through Si formed at the reaction interface.

A Kissinger plot for the estimation of activation energy for the process of silicon carbide formation is shown in Fig. 6(b), and the apparent activation energy has been calculated to be 255 ± 7.5 kJ/mol. This activation energy is much higher than the reported interdiffusion activation energy of Si and C, i.e., 12.98 kJ/mol.²⁰ The effect of heating rates on the SHS fabrication of TiC–Al₂O₃ from a TiO₂–Al–C mixture has shown that the SHS reaction is controlled by the diffusion of carbon through solid TiC.²¹ Similarly, the present SHS reaction involving the formation of SiC may be controlled by carbon diffusion through SiC as well. The formation of SiC has also been reported to be controlled by the formation of carbon-ion vacancies across the SiC layer.²² The self-diffusion of carbon in polycrystalline β -SiC has been studied by Hon *et al.*²³ and they report values of 841 ± 13.5 and 563 ± 8.7 kJ/mol for lattice and grain boundary diffusion, respectively. The activation energy for the self-diffusion of Si in β -SiC is also estimated to be 912 ± 4.8 kJ/mol.²⁴ This indicates that the diffusion of neither Si nor C through solid SiC is the rate-controlling factor in the present system. The activation energy of 240 ± 5 kJ/mol for the first exothermic peak is close to the second activation energy, indicating that the process of silicon carbide

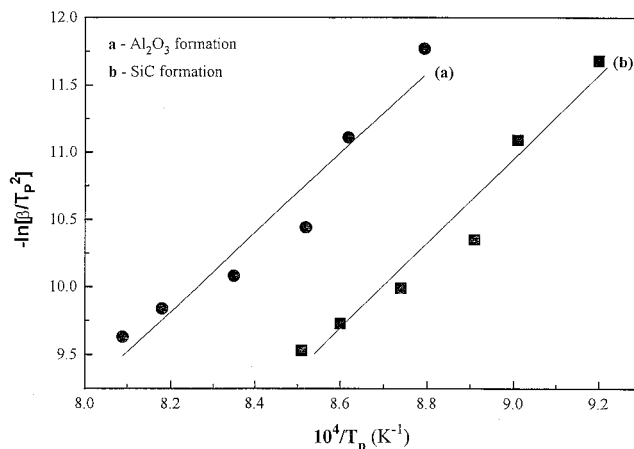


Fig. 6. Kissinger plots for the estimation of the activation energy of aluminothermic reduction of silica (a) and the formation of SiC (b).

formation is controlled by the liberation of Si in the aluminothermic reduction process. However, the contribution of chemical reaction between Si and C in controlling the overall reaction cannot be ruled out.

(3) X-ray and Microstructural Study

The XRD pattern of powder sample P₁ shows no evidence for the formation of Al₂O₃, Si, or SiC in the product, indicating the absence of any reaction during heat treatment. This is consistent with the thermoanalytical observations mentioned earlier. However, formation of Al₂O₃, Si, and SiC was detected in powder sample P₃, which was subjected to a higher heating rate (100°C/min). XRD analyses of the pellets show that unreacted SiO₂, as well as Al, is also present along with the reaction products (Al₂O₃ and SiC) after the SHS reaction, which supplements TG/DTA observations. Further, the presence of metallic Si in the product confirms that the reduction of SiO₂ has taken place by the aluminothermic route. From qualitative analyses using the peak intensities of the X-ray diffractograms, it appears that the amount of aluminum reacted during SHS decreases with an increase in the heating rates, as has been suggested earlier from the thermoanalytical studies. The relative intensity ratios also show a higher amount of SiC phase formation with an increase in the heating rates (Table III).

Figure 7 shows scanning electron microscopic images of samples C₇ and C₈. From the SEM images (Figs. 7(a) and (b)), it may be noted that formation of SiC whiskers is restricted to a relatively localized zone toward a particular surface instead of being distributed throughout the matrix. Similar observations have also been made for all of the pellet samples (C₂ through C₇). To identify the surface where whisker growth was favored, several TG/DTA supplementary experiments on pellets with marked surfaces were conducted at a heating rate of 20°C/min. It was identified that the surface touching the alumina crucible promotes whisker growth, whereas the other surfaces were free of any whiskers. The top and side surfaces of the samples being exposed to the flowing gas are

Table II. Details of the TG/DTA Analysis and Reaction Time during Heating Cycle

Sample	Mass gain (%)	Ratio of areas a and b	Al converted to alumina (%)	Al actually reacted during SHS (%)	Time interval between T _i and T _p (min)
C ₂	1.4	16.5	93.9	89.2	5.30
C ₃	1.3	14.0	92.8	88.1	2.92
C ₄	1.4	12.5	92.0	87.3	2.14
C ₅	1.3	11.7	91.4	86.7	1.6
C ₆	1.2	9.7	89.6	84.9	0.83
C ₇	1.2	9.7	89.6	84.9	0.71

Table III. Details of the XRD Analyses of Samples C_2 and C_7

Sample	Intensity of the peaks					Intensity ratio of the peaks		
	Si	SiO ₂	SiC	Al ₂ O ₃	Al	SiO ₂ /Si	SiC/Si	Al/Al ₂ O ₃
C_2	3196	375	364	1102	290	0.117	0.11	0.263
C_7	1516	356	393	1143	394	0.234	0.259	0.343

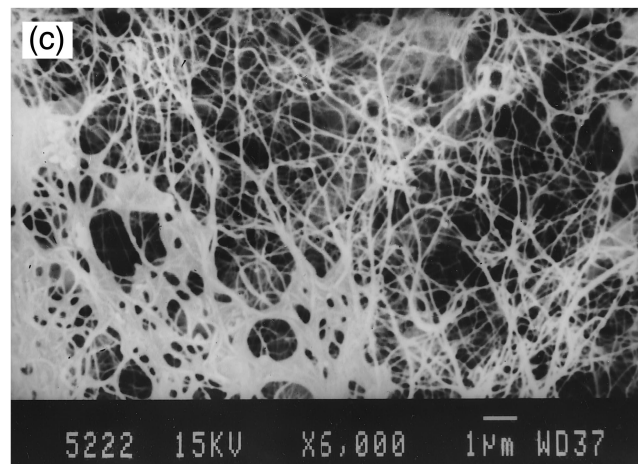
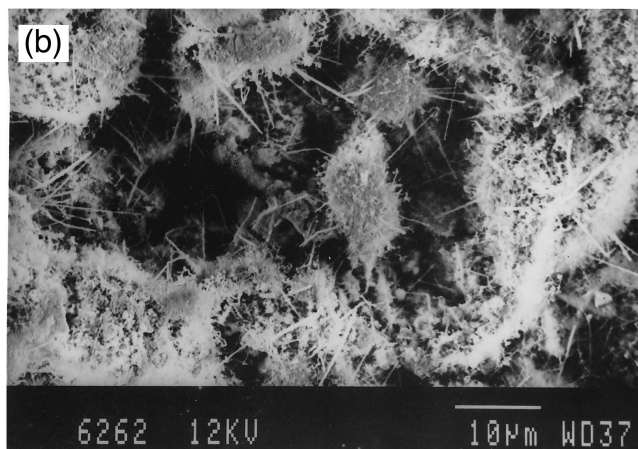
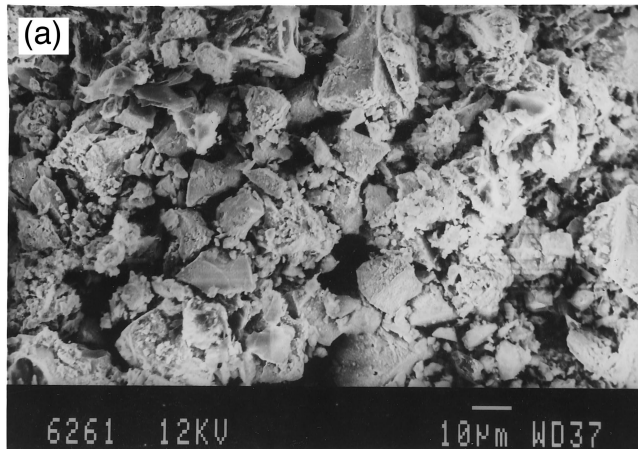


Fig. 7. SEM images of the two surfaces of pellet C_7 showing the formation of particulate in one surface (a) and formation of SiC whiskers in the other surface (b). Extensive growth of SiC whiskers in pellet C_8 (heated at 400°C/min) is shown in (c).

cooled by convection and radiation, whereas the bottom surface undergoes cooling only by conduction, and consequently, the heat transfer is expected to be much slower. The slow rate of heat transfer from the bottom surface of the pellets will enable the surface to remain at a relatively higher temperature for a longer period and that has possibly promoted the growth of SiC whiskers.

SEM images of sample C_8 heated at 400°C/min from room temperature to 1450°C and soaked for 10 min showed the formation of SiC whiskers throughout the sample and the quantity of whiskers was also found to be more (Fig. 7(c)). The formation of whiskers is known to be by either a vapor-phase or liquid-phase mass transfer process. The vapor-phase growth process is invariably associated with loss of mass and should have been reflected in the thermoanalytical studies. The absence of any significant mass loss during processing emphasizes the formation of SiC whiskers by the liquid-phase mass transfer process in the present investigation. The growth behavior of SiC whiskers in sample C_8 as observed in Fig. 7(c) suggests the above mechanism to be operative. The growth of whiskers also depends on the time. The absence of liquid Si for a sufficient length of time in the exposed surfaces of the pellets studied in TG/DTA has led to the formation of SiC particulates through the solid-state diffusion process, whereas the retention of liquid Si for longer periods of time in the bottom surfaces of pellets has helped in the formation of SiC whiskers.

IV. Conclusions

A systematic study on the effect of heating rates on the SHS formation of Al_2O_3 -SiC composites has been conducted. The powder mixture does not undergo any exothermic reaction at lower heating rates possibly because of poor contact between the reactants and segregation of liquid Al. The heating rates have shown a pronounced effect on both the reaction initiation temperature (T_i) and the peak temperature (T_p). Further, both T_i and T_p are found to increase with an increase in the heating rates. The reduction of silica is found to take place by the aluminothermic route and the exothermic reduction reaction is initiated only after melting of aluminum, suggesting reaction between solid silica and liquid aluminum. Three exothermic peaks due to aluminothermic reduction of silica, formation of SiC from the reaction of Si and C, and oxidation of Al, Si, or SiC have been observed. The conversion of aluminum marginally decreases with a gradual increase in the heating rates. The apparent activation energies for the aluminothermic reduction of silica and the formation of silicon carbide are estimated to be 240 ± 5 and 255 ± 7.5 kJ/mol, respectively. This indicates that possibly the diffusion of oxygen in the reaction interface is the rate-controlling factor for this present SHS process. The SEM results suggest that the formation of whiskers is possibly due to the liquid-phase mass transfer process.

Acknowledgment

We are thankful to Mr. Ravi Kumar for his help in carrying out the XRD studies during different stages of this investigation.

References

1. C. Wei and P. F. Becher, "Development of SiC Whisker Reinforced Ceramics," *Am. Ceram. Soc. Bull.*, **64** [2] 298-304 (1985).
2. T. N. Tieggs and P. F. Becher, "Sintered Al_2O_3 -SiC Whisker Composites," *Am. Ceram. Soc. Bull.*, **66** [2] 339-42 (1987).

- ³J. Homeny and W. L. Vaughn, "Silicon Carbide Whisker-Alumina Composites: Effect of Whiskers Surface Treatment on Fracture Toughness," *J. Am. Ceram. Soc.*, **73** [2] 394–402 (1990).
- ⁴J. Zhao, L. C. Stearns, M. P. Harmer, H. M. Chan, G. A. Miller, and R. F. Cook, "Mechanical Behavior of Alumina-Silicon Carbide 'Nanocomposites'," *J. Am. Ceram. Soc.*, **76** [2] 503–10 (1993).
- ⁵A. C. D. Chaklader, S. Das Gupta, E. C. Y. Lin, and B. Gutowski, "Al₂O₃-SiC Composites from Aluminosilicate Precursors," *J. Am. Ceram. Soc.*, **73** [8] 2283–85 (1992).
- ⁶H. M. Lee, H. L. Lee, and H. J. Lee, "Submicron Al₂O₃/SiC Composite Powder Preparation by SHS Technique," *J. Mater. Sci. Lett.*, **14**, 1515–17 (1995).
- ⁷R. A. Cutler, K. M. Rigrup, and A. V. Virkar, "Synthesis, Sintering, Microstructure and Mechanical Properties of Ceramics Made by Exothermic Reaction," *J. Am. Ceram. Soc.*, **75** [1] 36–43 (1992).
- ⁸D. Bandyopadhyay, L. C. Pathak, S. K. Das, I. Mukherjee, R. G. Ganguly, and P. Ramachandrarao, "Fabrication of Al₂O₃-SiC In-Situ Composites by a New Combustion Technique," *Mater. Res. Bull.*, **32** [1] 75–82 (1997).
- ⁹D. Bandyopadhyay, L. C. Pathak, S. K. Das, R. Kumar, and P. Ramachandrarao, "Synthesis of Ceramic Matrix Composites by RH-SHS"; pp. 599–604 in Proceedings of the International Conference on Recent Advances in Metallurgical Processes. Edited by D. H. Sastry, E. S. Dwarakadasa, G. N. K. Iyengar, and S. Subramanian. New Edge Publishing, Delhi, India, 1997.
- ¹⁰L. L. Wang, Z. A. Munir, and J. B. Holt, "The Combustion Synthesis of Copper Aluminides," *Metall. Trans.*, **21B**, 567–77 (1990).
- ¹¹W. C. Lee and S. L. Chang, "Ignition Phenomenon and Reaction Mechanisms of the Self-Propagating High Temperature Synthesis Reaction in the Titanium-Carbon-Aluminum System," *J. Am. Ceram. Soc.*, **80** [1] 53–61 (1997).
- ¹²H. C. Yi, A. Petric, and J. J. Moore, "Effect of Heating Rate on the Combustion Synthesis of Ti-Al Intermetallic Compounds," *J. Mater. Sci.*, **27**, 6797–806 (1992).
- ¹³Z. A. Munir, "Synthesis of High Temperature Materials by Self-Propagating Combustion Methods," *Am. Ceram. Soc. Bull.*, **67** [2] 342–49 (1988).
- ¹⁴N. P. Novikov, J. P. Borovinskaya, and A. G. Merzhanov; "Thermodynamic Analysis of Self-Propagating High-Temperature Synthesis Reactions"; pp. 174–87 in *Combustion Processes in Chemical Technology and Metallurgy*. Edited by A. G. Merzhanov. Institute of Chemical Physics, Chernogolovka, Russia, 1975.
- ¹⁵C. R. Bowen and B. Derby, "Self Propagating High Temperature Synthesis of Ceramic Materials," *Br. Ceram. Trans.*, **96**, 25–31 (1997).
- ¹⁶I. Barin and G. Platzki, *Thermochemical Data of Pure Substances*, 3rd ed. VCH Publishing, New York, 1995.
- ¹⁷A. Peng and Z. A. Munir, "The Effect of an Electric Field on Self-Sustaining Combustion Synthesis: Part II, Field Assisted Synthesis of β -SiC," *Met. Mater. Trans. B*, **26B**, 587–93 (1995).
- ¹⁸H. E. Kissinger, "Variation of Peak Temperature with Heating Rate in Differential Thermal Analysis," *J. Res. Natl. Bur. Stand. (U.S.)*, **57** [4] 217–21 (1956).
- ¹⁹C. Hass, "The Diffusion of Oxygen in Silicon and Germanium," *J. Phys. Chem. Solids*, **15**, 108–11 (1960).
- ²⁰R. Newmann and J. Wakefield, *Semiconductive Materials*; p. 201. Wiley-Interscience, New York, 1962.
- ²¹Y. Choi and S. W. Rhee, "Reaction of TiO₂-Al-C in the Combustion Synthesis of TiC-Al₂O₃ Composites," *J. Am. Ceram. Soc.*, **78** [4] 986–92 (1995).
- ²²H. Zhou and R. N. Singh, "Kinetics Model for the Growth of Silicon Carbide by the Reaction of Liquid Silicon with Carbon," *J. Am. Ceram. Soc.*, **78** [9] 2456–62 (1995).
- ²³M. H. Hon and R. F. Davis, "Self-Diffusion of ¹⁴C in Polycrystalline β -SiC," *J. Mater. Sci.*, **14**, 2411–21 (1979).
- ²⁴M. H. Hon, R. F. Davis, and D. E. Newbury, "Self-Diffusion of ³⁰Si in β -SiC," *J. Mater. Sci.*, **15**, 2073–80 (1980). □